Title
Selective corneal imaging using combined second-harmonic generation and two-photon excited fluorescence.

Journal
Optics Letters, 27(23)

ISSN
0146-9592

Authors
Yeh, Alvin T
Nassif, Nader
Zoumi, Aikaterini
et al.

Publication Date
2002-12-02

DOI
10.1364/ol.27.002082

Selective corneal imaging using combined second-harmonic generation and two-photon excited fluorescence

Alvin T. Yeh and Nader Nassif

Laser Microbeam and Medical Program, Beckman Laser Institute, University of California, Irvine, Irvine, California 92612

Aikaterini Zoumi and Bruce J. Tromberg

Laser Microbeam and Medical Program, Beckman Laser Institute and Center for Biomedical Engineering, University of California, Irvine, California 92612

Received June 12, 2002

A multiphoton microscope employing second-harmonic generation (SHG) and two-photon excited fluorescence (TPF) is used for high-resolution *ex vivo* imaging of rabbit cornea in a backscattering geometry. Endogenous TPF and SHG signals from corneal cells and extracellular matrix, respectively, are clearly visible without exogenous dyes. Spectral characterization of these upconverted signals provides confirmation of the structural origin of both TPF and SHG, and spectral imaging facilitates the separation of keratocyte and epithelial cells from the collagen-rich corneal stroma. The polarization dependence of collagen SHG is used to highlight fiber orientation, and three-dimensional SHG tomography reveals that approximately 88% of the stromal volume is occupied by collagen lamellae. © 2002 Optical Society of America

OCIS codes: 170.5810, 170.6930, 300.6410.

Biomedical imaging using multiphoton microscopy (MPM) is a rapidly growing field.[1,2] Most MPM studies employ two-photon excited fluorescence (TPF) to form images.[3] More recently, harmonic generation[4,5] and stimulated Raman[6,7] signals have been used to image cells and tissues. The nonlinear power dependence of these techniques confines image-forming signals to the focus of the laser beam, facilitating optical sectioning, and reduces sample photobleaching. For biological applications, near-infrared laser excitation minimizes scattering and absorption of the source, optimizing imaging in tissues at depth.

The MPM system used in this Letter employs a $Ti{:}Al_2O_3$ oscillator pumped by a frequency-doubled $Nd{:}YVO_4$ solid-state laser.[8] The 170-fs, 76-MHz mode-locked laser pulses are raster scanned across the sample by use of galvanometer-driven mirrors. Image-forming signals are collected by the focusing objective (Zeiss; 63× water immersion; N.A., 1.2) and directed via dichroic filters onto three detectors: two photomultiplier tubes to render *en face* images or the entrance slit of an imaging spectrometer coupled to a 16-bit slow scan CCD camera. Images are typically acquired with approximately 1–10-mW average power at the sample at a rate of approximately one (256×256) frame/s. Images presented in this Letter integrated at least 10 frames.

The cornea is composed of well-defined layers, including a surface of epithelial cells, the stroma, and an underlying endothelial layer. These layers of the cornea have been imaged by confocal microscopy using fluorescence from epithelial cells, keratocytes, and endothelial cells (for example, see Ref. 9). MPM has been used to image the metabolic state of the corneal epithelium.[10] Only ~5% of the stromal volume contains keratocytes, leaving most of the corneal structure uncharacterized by noninvasive optical methods.

The structural component in the cornea is predominantly extracellular collagen, approximately 15% of the stroma by weight.[11] Second-harmonic generation (SHG) from collagen was reported as early as 1971.[12] The resolution of MPM (~1 μm) permits imaging of corneal collagen lamellae composed of aligned collagen fibers or bundles. Fibers are composed of an ordered assembly of fibrils. Fibrils are the quaternary structure of collagen and require x-ray or electron microscopy for resolution of their structure.[13]

Immediately following euthanasia, rabbit eyes were enucleated and corneas surgically removed. Within minutes, a cornea was placed on a dry coverslip to be imaged via an inverted microscope. The spectra of nonlinear optical signals from a rabbit cornea are shown in Fig. 1. The spectrum in Fig. 1A was recorded when the laser was focused and scanned in the epithelium ($\lambda = 750$ nm). The corresponding MPM image of the corneal epithelium is shown in the inset. The scale bar represents 8 μm. The gray-scale image reveals dark nuclei in a cobblestone morphology of the epithelial layer with imaging signals originating from the cytoplasm of the cells. The spectrum of the imaging signals and its power dependence are typical of TPF from pyridine nucleotides (e.g., NADH).[14]

The spectrum in Fig. 1B was measured when the laser was focused and scanned in an acellular region of the corneal stroma ($\lambda = 800$ nm). The corresponding MPM stromal image is shown in the inset. Fine structure can be seen in the image, indicative of collagen fibers. These fibers are composed of an ordered array of collagen fibrils approximately 38 nm in diameter with an interfibrillar spacing of 60–70 nm.[15] The spectral line shape of the SHG signals from the stroma follows the laser spectrum and is

0146-9592/02/232082-03$15.00/0

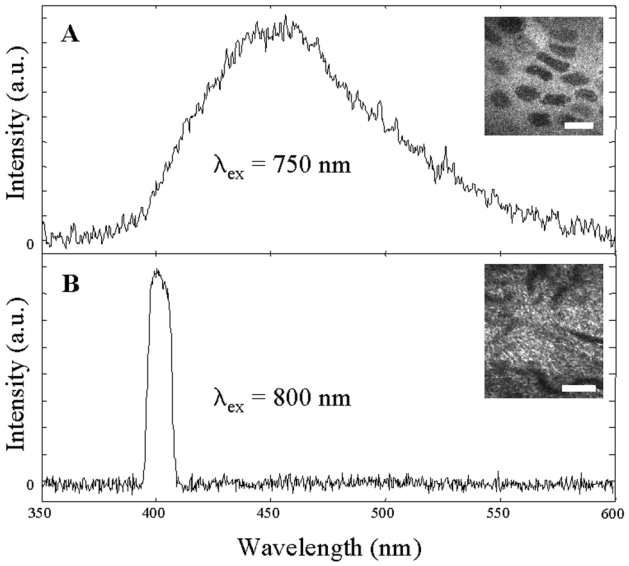

Fig. 1. Spectra of nonlinear optical signals generated in the cornea by multiphoton microscopy. A, Spectrum of cellular fluorescence following two-photon absorption from the epithelia with an incident laser wavelength of 750 nm. A representative image of the corneal epithelia is shown in the inset. B, Spectrum of SHG in the collagen matrix from an acellular region of the corneal stroma. A representative SHG image of an acellular region of the corneal stroma is shown in the inset. The incident wavelength is 800 nm. The scale bars represent 8 μm.

characteristically different from the cellular fluorescence spectrum shown in Fig. 1A. This upconverted signal can be tuned with the incident laser wavelength and has a quadratic dependence on the incident laser power.

A stack of SHG images used to form a three-dimensional (3-D) volume of the corneal stroma is shown in Fig. 2A. We acquired the image stack by changing the laser (λ = 800 nm) focus in 200-nm incremental steps. The 3-D reconstruction of the image stack reveals lamellae of collagen fibers lying predominantly parallel to the corneal surface. Domains of aligned collagen fibers are seen adjacent to other domains and voids, defined here as regions with no collagen fibers. To our knowledge, this is the first demonstration of nondestructive high-resolution imaging of normal corneal stroma without sectioning or the use of exogenous dyes. Figure 2B shows, at the same magnification, a hematoxylin and eosin (H&E) stained, *en face*, 6-μm histology section of the corneal stroma for comparison with the $x-y$ plane of the 3-D image stack. The $x-y$ plane of the image stack and the *en face* section in Fig. 2B have similar topographic features. However, the features seen in the 3-D image stack are more distinct because of the dark field illumination of MPM. Figure 2C shows a cross-sectional H&E stained section of the cornea. Large voids appear white in the pink matrix and are an artifact of histology. In the MPM image stack, voids are evident in the volume, possibly from stacking faults of the collagen lamellae. Three similar voids are marked by asterisks in the histology section in Fig. 2C. The volume fraction occupied by collagen lamellae is estimated from image analysis of the SHG signal in the 3-D tomographic reconstruction (Fig. 2A) to be ~88%.

Spectral filtering of the image-forming signals can be used to isolate cell and matrix components of the corneal stroma. The MPM images in Fig. 3 were taken in a rabbit cornea from a depth of ~180 μm with an incident laser wavelength of 800 nm. We tuned the incident laser wavelength to the red edge of the cellular TPF spectrum to minimize TPF from collagen. Shown in Fig. 3A is a MPM image of a portion of a keratocyte cytoplasm in its collagen matrix environment in the corneal stroma. The full extent of the cell and cellular processes is not visible in the optically thin imaging plane that is defined by the TPF and SHG signals. The cellular fluorescence can be seen because of metabolic activity,[10] possibly in response to stress induced by the enucleation and removal of the cornea. The cell can be imaged alone, as shown in Fig. 3B by spectral filtering of the image-forming

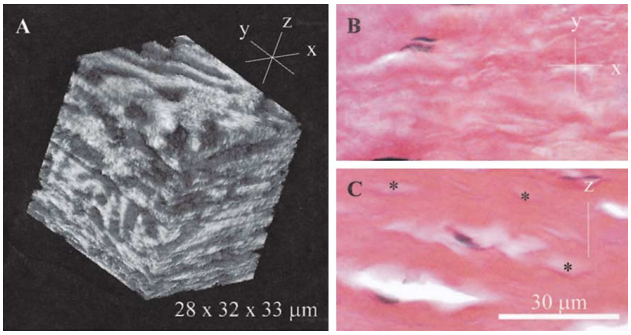

Fig. 2. A, Three-dimensional reconstruction of the corneal stroma from a stack of MPM images taken in 200-nm increments. B, H&E stained *en face* formalin-fixed section of the corneal stroma. C, H&E stained cross section of the corneal stroma. Asterisks demark voids similar to those seen in the MPM image stack of Fig. 2A.

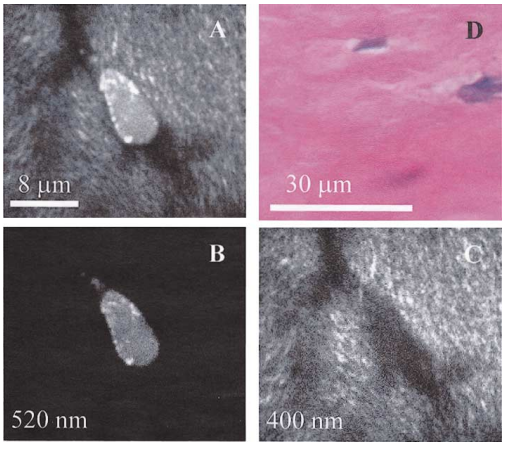

Fig. 3. Spectral filtering of biological components in the corneal stroma with an excitation wavelength of 800 nm. A, Image of a keratocyte in the corneal stroma from a depth of 180 μm. B, Isolation of the keratocyte from the collagen matrix by use of a bandpass filter at 520 nm. C, Imaging of the collagen matrix without the keratocyte by use of a bandpass filter at 400 nm. D, H&E stained *en face* section of the corneal stroma for comparison. The keratocytes appear blue in the histology.

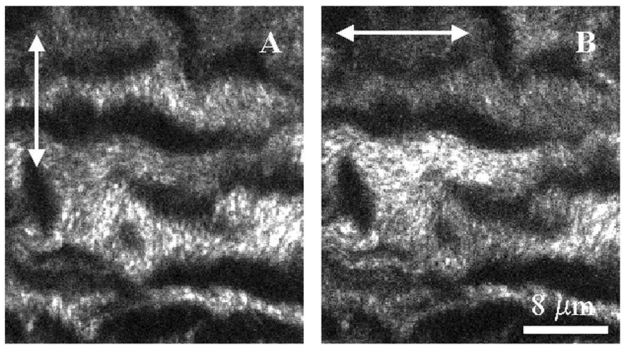

Fig. 4. Polarization dependence of SHG in the collagen matrix proteins of the corneal stroma. A, The relative intensity of the second harmonic is greater for fibers aligned in the vertical direction along the electric field of the laser. B, Multiphoton microscopy image of the same imaging plane by use of an orthogonal incident laser polarization.

signals with a bandpass filter within the cellular fluorescence spectrum (520 nm; see Fig. 1A). Similarly, the collagen matrix can be imaged without the cell by use of a bandpass filter at the second harmonic of the incident wavelength (400 nm) as shown in Fig. 3C. An *en face* H&E stained section is shown in Fig. 3D for comparison. Keratocytes are stained blue and appear to have a similar morphology to that seen in the MPM images.

The sensitivity of SHG in collagen to the polarization of the incident laser ($\lambda = 800$ nm) is illustrated in Fig. 4. The second-order polarizability of collagen has been shown to be dominated by a single axial component aligned along the fiber axis.[16] In recent work a transmitted second-harmonic signal from a porcine cornea was used to map collagen fiber orientation.[17] The images in Fig. 4 are from the same imaging plane at a depth of 30 μm into the corneal stroma. The general structural features are common to both the images, with differences in the relative intensity of the features distinguishing the two images. These differences are the result of different orientations of the collagen fibers relative to the electric field polarizations. Vertically (horizontally) oriented fibers in the image are preferentially highlighted in Fig. 4A (4B). The SHG intensity of the features in the images is dependent on the orientation of the collagen fiber relative to the electric field of the laser.

The images presented in this Letter show the promise of MPM as a nondestructive technique to image the corneal cells and stromal collagen without sectioning or staining. These results outline a general strategy to use MPM for the study of cell–cell and cell–matrix interactions in a broad range of biological systems. Although not specifically investigated in this work, the unique sensitivity of MPM suggests the potential of the technique to monitor noninvasively the state of health of the cornea. Possible applications of this technology could include detecting and tracking the progression of corneal pathologies as well as monitoring the effect of surgical procedures such as corneal transplantation and refractive surgery.

This work was supported by the National Center for Research Resources at the National Institutes of Health (Laser Microbeam and Medical Program, RR-01192), the U.S. Air Force Office of Scientific Research, Medical Free-Electron Laser (F49620-00-1-0371), and a National Institutes of Health Carcinogenesis Training Grant (CA-09054) to A. T. Yeh (e-mail: ayeh@laser.bli.uci.edu).

References

1. R. M. Williams, W. R. Zipfel, and W. W. Webb, Curr. Opin. Chem. Biol. **5,** 603 (2001).
2. K. Konig, J. Microsc. (Oxford) **200,** 83 (2000).
3. W. Denk, J. H. Strickler, and W. W. Webb, Science **248,** 73 (1990).
4. P. J. Campagnola, A. C. Millard, M. Terasaki, P. E. Hoppe, C. J. Malone, and W. A. Mohler, Biophys. J. **81,** 493 (2002).
5. Y. Guo, P. P. Ho, H. Savage, D. Harris, P. Sacks, S. Schantz, F. Liu, N. Zhadin, and R. R. Alfano, Opt. Lett. **22,** 1323 (1997).
6. J.-X. Cheng, A. Volkmer, L. D. Book, and X. S. Xie, J. Phys. Chem. B **105,** 1277 (2001).
7. E. O. Potma, W. P. de Boeij, P. J. M. Haastert, and D. A. Wiersma, Proc. Nat. Acad. Sci. USA **98,** 1577 (2001).
8. A. Agarwal, M. L. Coleno, V. P. Wallace, W.-Y. Wu, C.-H. Sun, B. J. Tromberg, and S. C. George, Tissue Eng. **7,** 191 (2001).
9. M. Bohnke and B. R. Masters, Prog. Retinal Res. **18,** 553 (1999).
10. D. W. Piston, B. R. Masters, and W. W. Webb, J. Microsc. (Oxford) **178,** 20 (1995).
11. D. M. Maurice, in *The Eye*, H. Davison, ed. (Academic, Orlando, Fla., 1984), pp. 1–158.
12. S. Fine and W. P. Hansen, Appl. Opt. **10,** 2350 (1971).
13. K. M. Meek and N. J. Fullwood, Micron **32,** 261 (2001).
14. S. Huang, A. A. Heikal, and W. W. Webb, Biophys. J. **82,** 2811 (2002).
15. K. M. Meek and A. J. Quantock, Prog. Retinal Res. **20,** 95 (2001).
16. P. Stoller, B.-M. Kim, A. M. Rubenchik, K. M. Reiser, and L. B. Da Silva, J. Biomed. Opt. **7,** 1 (2002).
17. P. Stoller, K. M. Reiser, P. M. Celliers, and A. M. Rubenchik, Biophys. J. **82,** 3330 (2002).